

# THE ROLE OF LOCALIZED ROUGHNESS ON THE LAMINAR-TURBULENT TRANSITION ON THE OBLIQUE WING

S.N. Tolkachev\*, V.N. Gorev\*, V.V. Kozlov\*

\*Khristianovich Institute of Theoretical and Applied Mechanics SB RAS

## Abstract

*The combination of hot-wire measurements and liquid crystal thermography techniques is used, which allowed to investigate stationary disturbances development from the stage of excitement to the turbulence. A position of maximal receptivity to the surface roughness was found. It is shown that cylindrical roughness element induces the pair of counter-rotating vortices, modifying a boundary layer structure. Near the vortex core favorable conditions for secondary disturbances are formed, the development of which lead to a laminar-turbulent transition. These disturbances are sensitive to acoustic field, so can be investigated by technique of controlled disturbances. The appearance of additional stationary disturbances in conditions of high-amplitude acoustics was observed.*

## 1 Introduction

The aircraft producers are competing for the lowest air drag of the plane. Every percent is on account, so the laminarization of the flow around the airplane has a good potential. Modern ones fly on transonic speed, so they use the swept wings.

The main reason for the laminar-turbulent transition on the flat plate and straight wing is the development of Tollmien-Schlichting waves. The effective way to suppress them is to prolong the favorable pressure gradient region.

The laminar-turbulent scenario on the swept wing is complimented by cross-flow instability mechanism because of freestream velocity and pressure gradient directions

mismatch and viscous effects lead to the three-dimensional structure of the boundary layer. It is easy to highlight the longitudinal and transversal velocity components. The second one has the inflection point in the favorable pressure gradient region. This point is connected to the cross-flow instability, which usually has a shape of longitudinal vortices which modify the boundary layer structure [1]. This process creates the favorable conditions for the secondary disturbances appearance and development [2, 3] and, finally, to the laminar-turbulent transition.

This work is oriented on the investigation of laminar-turbulent transition in the favorable pressure gradient region caused by the roughness elements due to the secondary instability mechanism.

## 2 Experimental conditions

Experiment carried out in the low-turbulent wind tunnel AT-324 of Khristianovich Institute of Theoretical and Applied Mechanics. The test section size is 1000×1000×4000 mm. The freestream velocity controlled by Pitot-static tube, connected to the micromanometer and depending on the tasks changed in interval. The level of the turbulence didn't exceed the 0.03%. The temperature of oncoming air was about 293°K.

There were two investigation techniques used hot-wire measurements and liquid crystal thermography. The second one needed the ohmic heater to provide the process of heat exchange and because the operating temperature interval of liquid crystal film was 303-306°K. Investigations [4] showed that weak heating

don't have sufficient influence on the phenomena in boundary layer.

Hot-wire data consist of samples in each space point. Each sample had a duration 1 second and contained 10000 time points. This data was processed using MathWorks Matlab. To receive characteristics of stationary processes averaging was used. Velocity pulsations were analyzed using fast Fourier transform.

For investigations the swept wing model was made of perspex with a chord of  $C_h = 400$  mm and sweep angle  $45^\circ$  with a possibility for changing the angle of attack (Fig.1.). The airfoil consists of cylinder with diameter of 80 mm and two converged plates. The disturbances developing on the test section walls cut by the end plates.

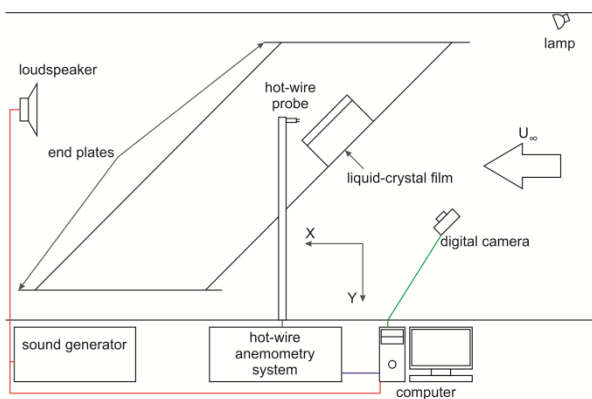


Fig. 1. Scheme Of Experiment For Investigation The Cross-Flow Instability And Secondary Instability.

Longitudinal vortices excited by the one of the three cylindrical roughness elements with a height 0.4, 0.7 and 1 mm and 1.6 mm diameter. Secondary disturbances excited by the loudspeaker, placed in diffusor of the wind tunnel. The freestream velocity was in range  $U_\infty = 6.8 - 14.6$  m/s. The angle of attack was  $-7.2^\circ$ . To suppress the shedding phenomena on

the down side of the airfoil the turbulators was placed in the position of maximal thickness.

### 3 Experimental results

Hot-wire measurements over the boundary layer of upper surface of the wing showed the realization of favorable pressure gradient region, which is necessary to suppress the development of Tollmien-Schlichting waves (Fig.2.).

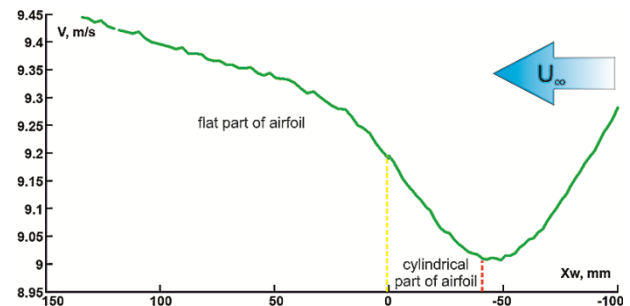


Fig. 2. Velocity Distribution Over The Upper Surface Of The Wing.

Freestream velocity:  $U_\infty = 10.4$  m/s

Visualization patterns reveal the formation behind the roughness element a couple of counterrotating vortices one of which decays fast along the flow, because the direction of its rotation is opposite to the cross-flow.

The liquid crystal thermography allowed comparing the stationary disturbances excitation by the roughness elements of different heights (Fig. 3.) in one pattern. So it is quite convenient to compare different velocity regimes. In favorable conditions (small roughness element or low velocity) it is quite hard to find stationary structures behind the single roughness element, there is no fast disturbance growing. The increase of roughness size or/and freestream velocity lead to the appearance of saturated nonlinear stationary structure, on which the additional stationary structures are born.

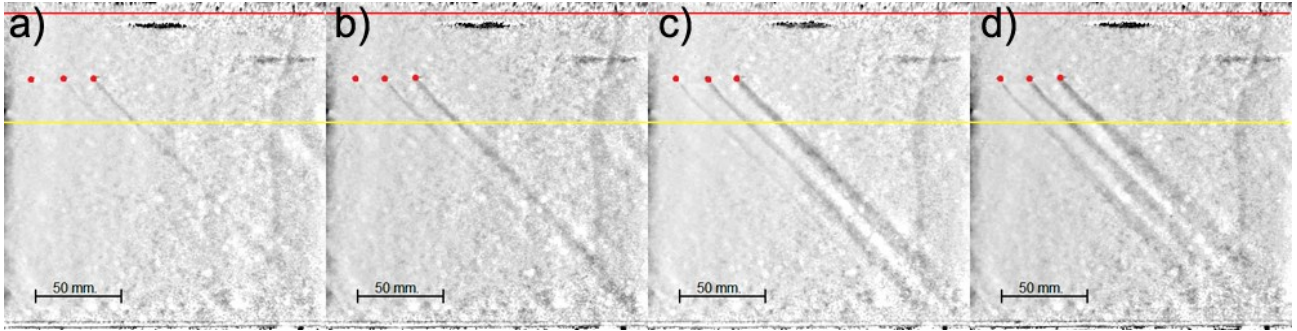


Fig. 3. Visualization Patterns Of Stationary Boundary Layer Structure Behind The Roughness Elements.

Roughness elements heights are: 0.4 mm, 0.7 mm, 1 mm. The roughness element position is  $\theta = 55.1^\circ$ . The freestream velocity: a)  $U_\infty = 6.8$  m/s, b)  $U_\infty = 9.2$  m/s, c)  $U_\infty = 11.8$  m/s, d)  $U_\infty = 14.6$  m/s

Liquid crystal visualizations allowed to choose the regime for hot-wire investigations:  $U_\infty = 10.4$  m/s, the roughness element with height 0.7 mm on the position  $\theta = 55.1^\circ$ .

Hot-wire measurements in transversal direction near the position of cylindrical airfoil part to flat joint shows the presence of two

counterrotating vortices. In the position between the defect and exceeding of velocity that is near the stationary vortex core the high-frequency wavepacket appears (Fig. 4.). This connection to the stationary vortex allow to assume the secondary instability mechanism is a reason for the wavepacket onset.

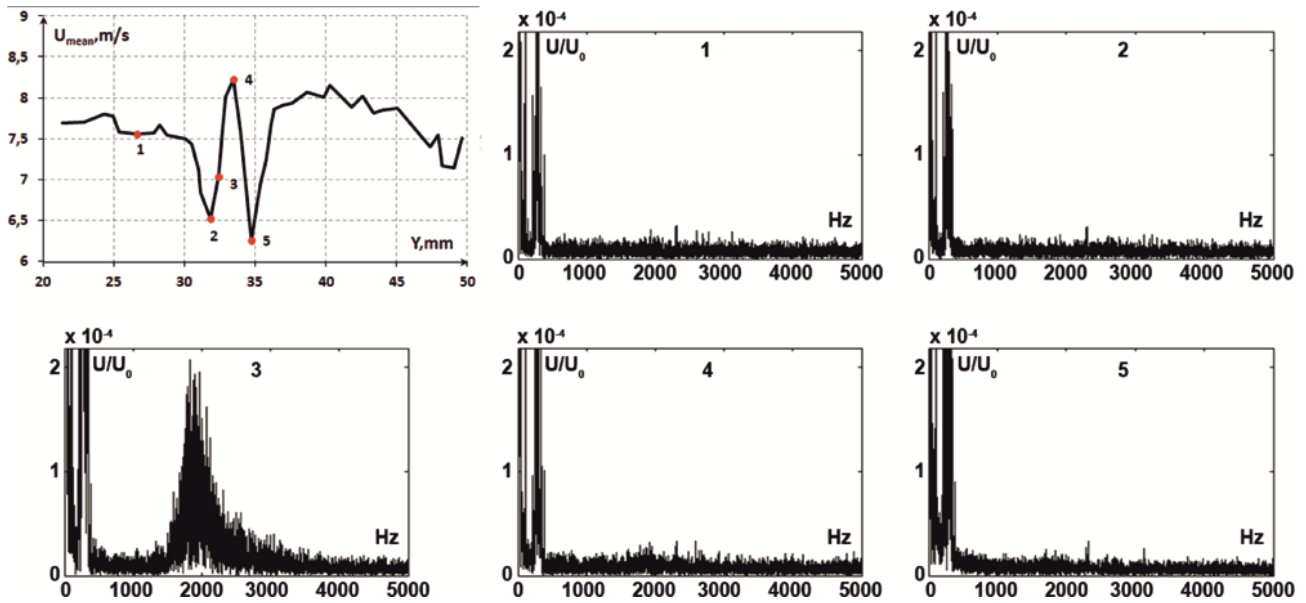


Fig. 4. Hot-Wire Results In Transversal Direction.

Velocity distribution for  $H = 0$  mm and spectra in five space points.

Hot-wire measurements in the other sections shows the most intensive secondary disturbance development is near the stationary vortex core. In these positions (Fig. 5.) the influence of freestream velocity on the secondary disturbance development scenario was investigated.

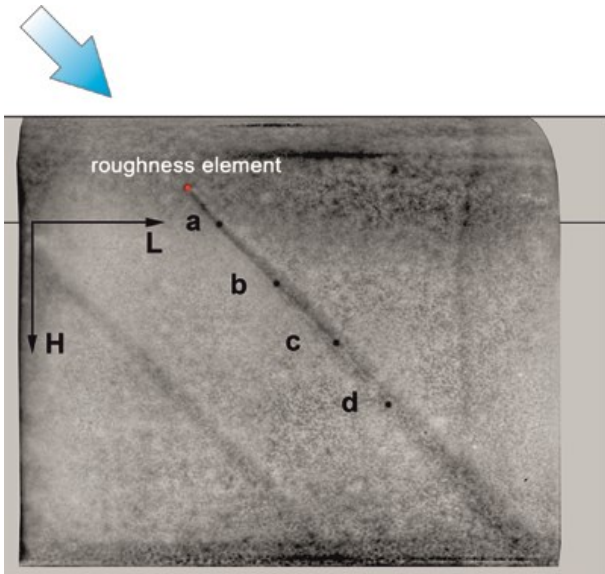


Fig. 5. Positions Of Hot-Wire Measurements On The Model Of The Wing.

On low velocity (in our experimental conditions 7.7 m/s) there are no secondary disturbances (Fig. 6.).

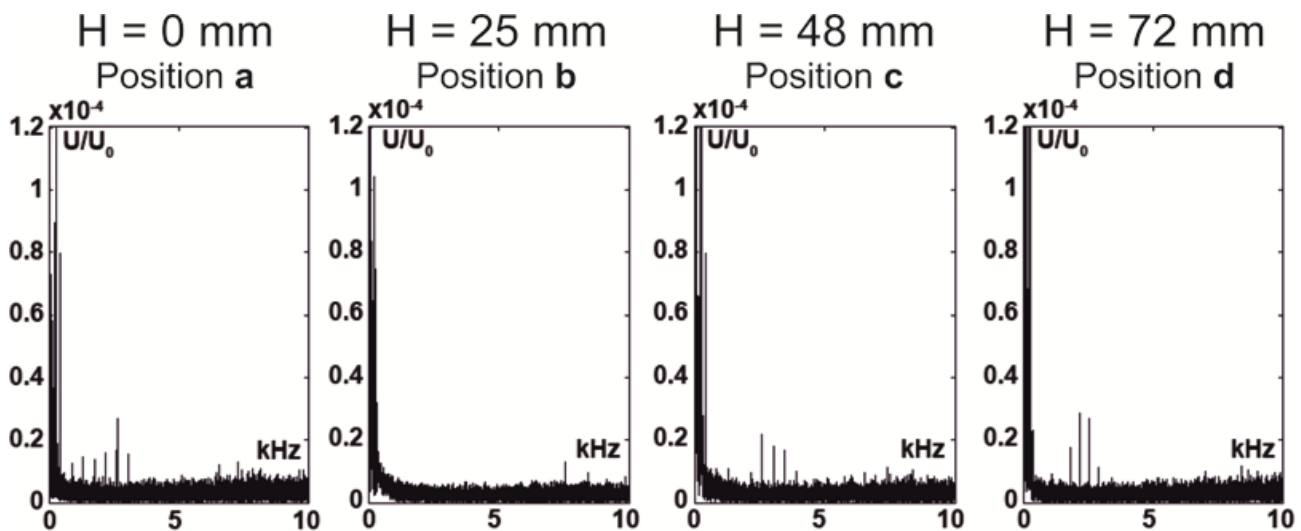


Fig. 6. Velocity Spectra Near The Stationary Vortex Core For  $U_\infty = 7.7$  m/s.

The increase of freestream velocity up to 10.4 m/s leads to appearance of wavepacket, the development of which goes through the several stages: linear development (Fig. 7. Position a, Position b), on which the spectrum shape almost

not changes, only the amplitude and frequency interval floats. The nonlinear stage can be characterized by filling of low-frequency part of the spectrum (Fig. 7. Position c), which leads to the turbulent flow regime (Fig. 7. Position d).

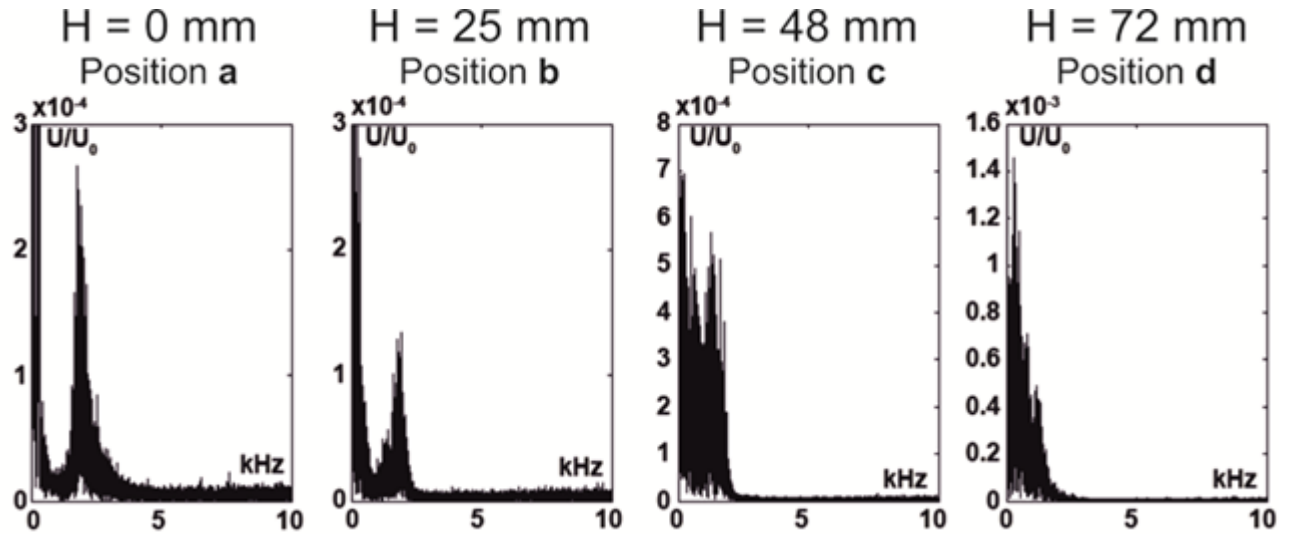


Fig. 7. Velocity Spectra Near The Stationary Vortex Core For  $U_\infty = 10.4$  m/s.

The further increase of freestream velocity up to 13.2 m/s enables the additional mechanism – the appearance of harmonics of main frequency interval (Fig. 8. Position a,

Position b). This mechanism probably enables, if the disturbance amplitude become higher than  $0.01 U_\infty$ . Finally it leads to the turbulent flow regime (Fig. 8. Position c, Position d).

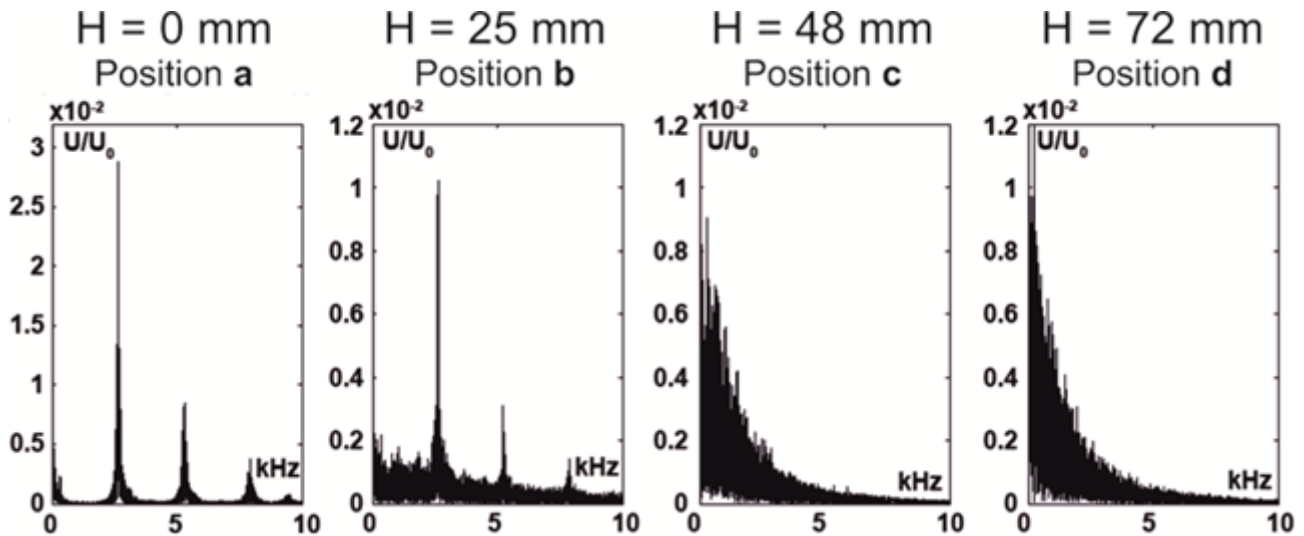


Fig. 8. Velocity Spectra Near The Stationary Vortex Core For  $U_\infty = 13.2$  m/s.

One of the most important tasks for airfoil design is to determine the position of maximal receptivity to the roughness position. For this purpose two techniques were tested.

The first one is hot-wire measurements in fixed measurement grid, which contains the disturbed and undisturbed regions of boundary layer. For each roughness position (Fig. 9.) the integral characteristics were calculated.

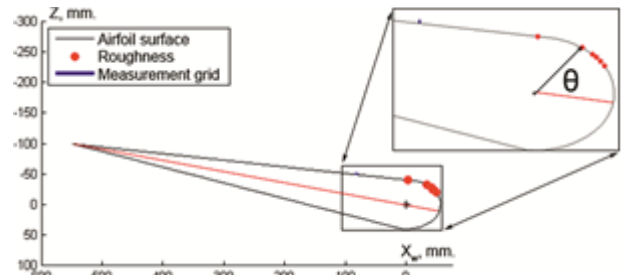


Fig. 9. Roughness Element Positions For Receptivity Investigation

The receptivity of stationary disturbance to the roughness position the value  $A_{Stat}$  was used.

$$A_{Stat} = \int_{S_{meas}} (U_0 - U_{undist})^2 dS \quad (1)$$

where:

$U_0$  - mean velocity in the measurement position;

$U_{undist}$  - velocity in the same position in undisturbed case;

$S_{meas}$  - measurement area.

The receptivity of secondary disturbances was characterized by value  $A_{Sec}$ :

To characterize secondary disturbances the integral of velocity spectra pulsations in

$$A_{Sec} = \int_{S_{meas}} \int_{\nu=100Hz}^{10000Hz} \tilde{U}(\nu) d\nu dS \quad (2)$$

where:

$\tilde{U}(\nu)$  – velocity in Fourier space in the measurement position;

$\nu$  – frequency;

$S_{meas}$  - measurement area.

The frequency interval 100-10000 Hz was chosen to avoid electrical noise and probe vibrations.

To have a possibility of comparing the position of maximal receptivity for different types of instability these integral values were normalized by 1. The experimental result is on the **Fig. 10**. The position of maximal receptivity of stationary disturbances is near  $\theta = 58^\circ$ . The position of one of secondary disturbances differs and lies near the  $\theta = 70^\circ$ .

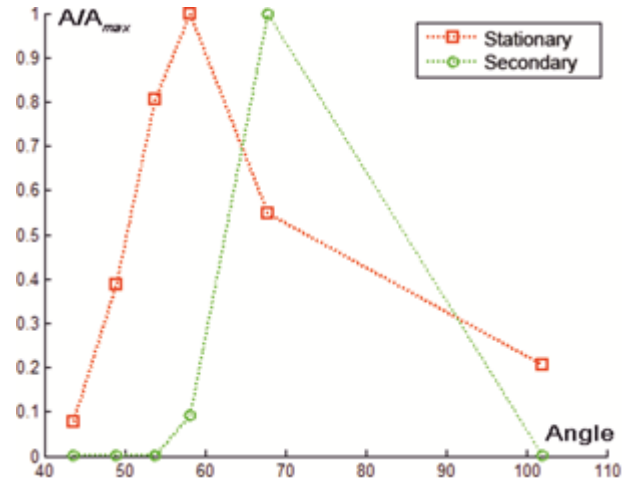


Fig. 10. Receptivity Value Distributions For Stationary And Secondary Disturbances Depending On The Roughness Element Position.

The second approach for determine the position of maximal receptivity used the liquid crystal thermography. High level of longitudinal disturbances localization allowed placing several roughness elements on the leading edge of the swept wing to determine the position maximal receptivity by one visualization pattern. The experimental results are in **Fig. 11**. These results are in a good agreement with a result of hot-wire measurements and required less time. The position of maximal receptivity is near  $\theta = 55.1^\circ$ .

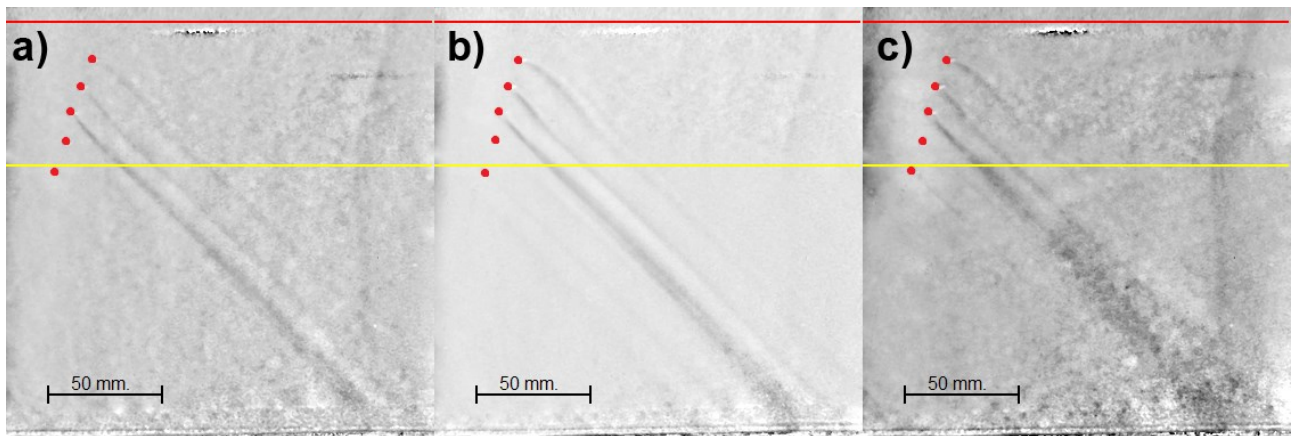


Fig. 11. Visualization Patterns Of Stationary Boundary Layer Structure Behind The Separated Roughness Elements On Different Locations From The Line Of Airfoil Symmetry (red).

The freestream velocity: a)  $U_\infty = 9.2$  m/s, b)  $U_\infty = 11.8$  m/s, c)  $U_\infty = 14.6$  m/s. The roughness element positions:  $\theta = 22^\circ$ ,  $\theta = 41.3^\circ$ ,  $\theta = 55.1^\circ$ ,  $\theta = 74.4^\circ$  and on the flat part near the airfoil cylindrical part to flat joint.

Particular question was about the additional stationary structures appearance. Using high-amplitude acoustics with frequency only from interval of natural wavepacket this effect was observed (Fig. 12.), so it is the result of nonlinear development of secondary disturbances.

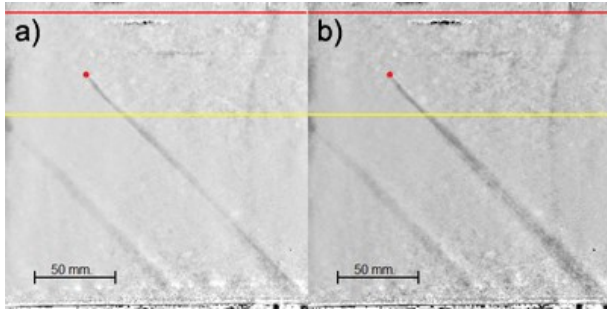


Fig. 12. Visualization Patterns Of Stationary Boundary Layer Structure Behind The Separated Roughness Element.

The freestream velocity is  $U_\infty = 10.4$  m/s. The roughness element position is  $\theta = 55.1^\circ$ . The acoustic excitation regime: a) without acoustic excitation, b) with high-amplitude acoustics with frequency 1500 Hz.

The development of one mode of secondary instability was investigated using the method of controlled disturbances. For this purpose hot-wire measurements along the stationary vortex core were carried out.

Analysis of amplitude data showed the exponential growing on initial stage until the amplitude of secondary instability less than  $0.01 U_\infty$  (Fig. 13.). In the position  $X_w = 61$  mm the disturbance saturates.

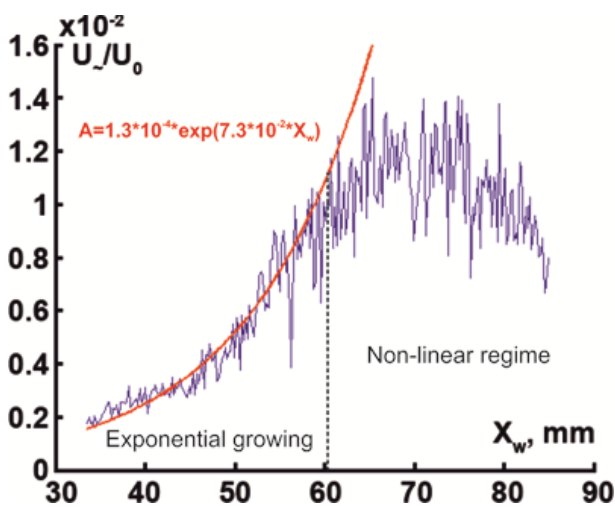


Fig. 13. The Development Of Secondary Disturbance Amplitude Along The Flow.

The interesting result is the sharp change of phase velocity from  $0.55U_\infty$  up to  $0.63U_\infty$  (Fig. 14.) in the position of changing disturbance state  $X_w = 61$  mm.

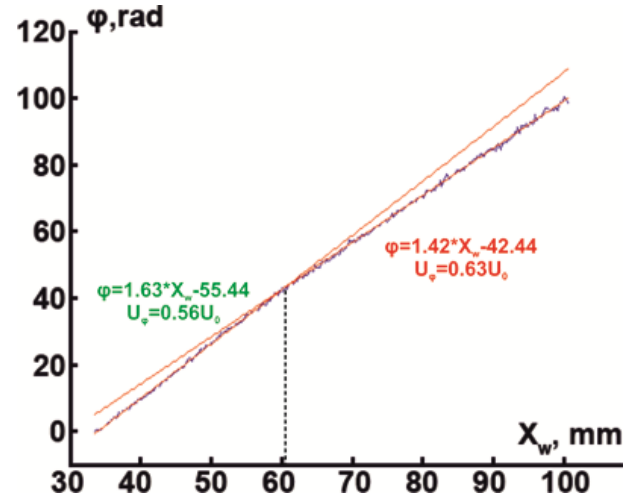


Fig. 14. Change Of Phase Velocity Of Excited Mode Of Secondary Instability.

#### 4 Conclusion

In this work the process of laminar-turbulent transition, driven by cylindrical roughness element was observed. The technique of discovering the position of maximal receptivity to the roughness on the leading edge of the swept wing is suggested.

It is found, that laminar-turbulent-transition on the leading edge of the swept wing caused by the development of high-frequency disturbances of secondary instability, which appear near the stationary vortex core and has a form of wavepacket.

Depending on the freestream velocity the scenario of transition consist of different nonlinear mechanisms. In low velocity regime low-frequency part of the spectrum is filling. On higher velocity the mechanism of appearing harmonics enables.

Nonlinear effects of secondary disturbances could lead to the appearance of additional stationary structures. This process is one of the mechanisms of expansion the area with turbulent regime.

The method of controlled disturbances allowed receiving the quantitative data about separate mode of secondary disturbance development. It was observed the connection

between the saturation of disturbance growing and increase of phase velocity.

## References

- [1] Orszag S.A., Patera A.T. Secondary instability of wall-bounded shear flows. *J. Fluid Mech.*, Vol. 128, pp. 347 – 385, 1983.
- [2] Kohama Y. Some expectation on the mechanism of cross-flow instability in a swept-wing flow *Acta Mech.* Vol. 66, pp. 21 – 38, 1987.
- [3] Kozlov V.V., Levchenko V.Ya., Sova V.A., Shcherbakov V.A. Acoustic field effect on laminar turbulent transition on a swept wing in the favourable pressure gradient region *Fluid Dynamics*, Vol. 38, No. 6, pp. 868 – 877, 2003.
- [4] Brylyakov A.P., Zharkova G.M., Zanin B.Yu., Kovrizhina V.N., Sboev D.S. Effect of free-stream turbulence on the flow structure near a wedge and the windward side of an airfoil. *Journal of Applied Mechanics and Technical Physics*. Vol. 45, Issue 4, pp. 510 – 516, 2004.

## Contact Author Email Address

Tolkachev Stepan  
<mailto:tolkachevst@gmail.com>

Kozlov Viktor  
<mailto:kozlov@itam.nsc.ru>

## Copyright Statement

The authors confirm that they, and/or their company or organization, hold copyright on all of the original material included in this paper. The authors also confirm that they have obtained permission, from the copyright holder of any third party material included in this paper, to publish it as part of their paper. The authors confirm that they give permission, or have obtained permission from the copyright holder of this paper, for the publication and distribution of this paper as part of the ICAS 2014 proceedings or as individual off-prints from the proceedings.